A Shaped-Reflector High-Power Converter for a Whispering-Gallery Mode Gyrotron Output

Jeffrey A. Lorbeck, *Member, IEEE*, and Ronald J. Vernon, *Member, IEEE*

Abstract—**A dual-shaped dual-reflector synthesis technique is applied to the design of a quasi-optical antenna system in a high-power microwave application for which the primary radiator is not conveniently described as a point source (spherical constant-phase surface). In addition, the output beam is required to be focused, and neither the entrance nor the exit pupil is conveniently described as being circular. The synthesis technique developed in this paper is a generalization of a well-established method which has found widespread application in the design of dual-shaped reflectors for satellite communication, radio astronomy, etc. Removing the usual assumptions of point-source illumination and parallel-ray output, as well as circular entrance and exit pupils, however, leads to expressions which may find application in a broader class of shaped-reflector designs. A reflector system has been designed using the general synthesis procedure which we have developed. The system transforms the right-hand rotating $TE_{15,2}$ mode propagating in 50.8 mm (2 in) diameter circular waveguide at 110 GHz into the HE_{11} mode in 31.8 mm (1-1/4 in) diameter corrugated waveguide. A brief description of the experimental verification of the device performance is given.**

I. Introduction

ELECTRON-CYCLOTRON resonance heating (ECRH) used in fusion plasma experiments requires sources of microwave energy in the frequency range of about 50 to 150 GHz. High-power (~0.5 to 1.0 MW) microwave tubes called gyrotrons are currently under development to meet the demands of these experiments. A certain class of gyrotrons operates in a so-called whispering-gallery mode (WGM) defined here as a rotating TE_{mn} circular waveguide mode for which the azimuthal index m is much greater than the radial index n, and n is small (m >> n, n = 1 or 2). The mode is said to be rotating since its azimuthal dependence varies as exp(-jmϕ) instead of a sin($m\phi$) or cos(mϕ) dependence that one would find for an azimuthally stationary mode.

Although the WGM is desired for excitation in the interaction cavity of the gyrotron (the so-called asymmetric volume modes, a closely related class of modes for which the techniques introduced below may equally well be applied, have also been used), its broad radiation pattern from an open-ended waveguide and its complex polarization make it unsuitable for direct use in plasma heating experiments. More efficient use of the microwave energy can be realized with a well-collimated, linearly-polarized beam (the polarization can then be manipulated as desired with a twist reflector).

A simple quasi-optical reflector system to transform the WGM into a low-order free-space mode was first proposed by Vlasov *et al.* over two decades ago [1]. The output of these earliest devices had high-polarization purity, although they exhibited poor output power distributions due to diffraction effects. Several improved designs of the original reflector system have been reported (e.g., [2], [3]). These designs have generally not fully exploited the powerful 3-D geometrical-optics (GO) based dual-shaped dual-reflector surface-synthesis techniques, however, that have proven highly successful for antenna systems used in satellite communication, radio-astronomy, etc.

In this paper we recast a dual-shaped dual-reflector GO-based synthesis technique reported by Galindo-Israel, *et al.* [4] into a form which allows for arbitrary input and output distributions of the power and phase. In particular, we no longer assume spherical input constant-phase surfaces for which the primary radiator may be treated as a point source, nor are we able to accurately model the primary-radiator directive gain with a simple azimuthally-symmetric $\cos^q$ pattern. At the output of the system of reflectors, we generally require constant-phase surfaces which are not planar. In addition, we have found it most convenient to describe the input and output surfaces and power and phase distributions over rectangular domains so neither the input nor the output pupil is necessarily circular. The generalizations which we describe may become increasingly important as the applications for quasi-optical techniques continue to grow.

This paper is organized as follows: the GO-ray picture of the propagation of the WGM is reviewed in Section II; a generalized dual-shaped dual-reflector synthesis technique is developed in Section III; details of an actual reflector design are provided in Section IV; experimental investigation of the reflector system is presented in Section V; concluding remarks are given in Section VI.

II. GO Rays for a WGM

Since the synthesis technique which we have developed is GO based, the radiation of the WGM from the circular waveguide must be described in terms of GO rays. The GO ray picture of WGM field propagation in a circular-cylindrical waveguide has been outlined in [5]. According to this GO model, a section of the wall of angular extent equal to $2\theta_w = 2 \arccos(m/\chi'_{mn})$, where m is the azimuthal index of the mode and χ'_{mn} is the nth nonzero root of the equation $J'_m(x)$

Manuscript received March 1, 1993; revised July 18, 1994. This work was supported by the Magnetic Fusion Energy Technology Fellowship which is administered for the U.S. Department of Energy (D.O.E.) by Oak Ridge Associated Universities and under a University of Wisconsin Graduate School Fellowship and by U.S.D.O.E. Contract DE-FG02-85ER52122.

The authors are with the University of Wisconsin at Madison, Department of Electrical and Computer Engineering, Madison, WI 53706 USA.

IEEE Log Number 9415636.

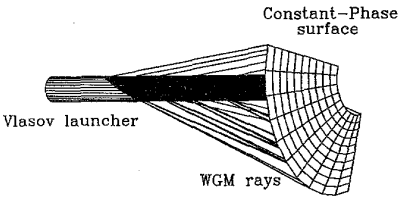

Fig. 1. Constant-phase surface of a WGM (TE $_{15,2}$ mode in 2 in (5.08 cm) diameter waveguide at 110 GHz, $\rho_{mn} = 0.68a$) radiating into free space from the Vlasov launcher.

$= 0$, may be removed from the circular waveguide to allow the WGM to radiate completely into free space. A ray diagram assuming the right-hand rotating $TE_{15,2}$ mode in 50.8 mm (2") diameter waveguide at 110 GHz is shown in Fig. 1. Given this diameter and frequency, one may show that 873 modes (not including the two-fold azimuthal rotation degeneracies) can be supported in the 50.8 mm diameter waveguide with the $TE_{15,2}$ mode being associated with the 128th eigenvalue.

Note from Fig. 1 that a point-source model of the radiation from the waveguide with a section of wall removed (a structure which we refer to as the Vlasov launcher) would be highly inappropriate in the vicinity of the aperture where the first reflector will be placed. In addition, the input pupil boundary is not conveniently described as being circular, nor does the field possess the circular symmetry observed for radiation from a simple horn antenna used with lower-order modes. The complex nature of the field emitted by the primary radiator, the Vlasov launcher, would not permit immediate application of the synthesis techniques which have appeared in the literature on reflector antennas. The development appearing below is thus a recasting of the expressions which govern the surface synthesis so that a more general primary radiator may be allowed.

Ultimately we wish to couple the reflector-system output into a lower-order waveguiding environment (we used a 1-1/4 in corrugated waveguide which supports the balanced HE_{11} mode) so that a focused output beam is indicated. The governing equations of the synthesis routine are sufficiently general to allow for focused output in distinction with the more typical parallel-ray output.

III. Generalized Dual-Shaped Reflector Synthesis

Consider an arbitrary three-dimensional (3-D) reflector system comprised of an input constant-phase surface, subreflector, main reflector, and output constant-phase surface with vectors $\boldsymbol{R}_I$, $\boldsymbol{R}_S$, $\boldsymbol{R}_M$, and $\boldsymbol{R}_O$, respectively, defining each surface (see Fig. 2). The ray path from the input constant-phase surface to the subreflector will be denoted by the vector $\boldsymbol{I}$, from the subreflector to the main reflector by the vector $\boldsymbol{S}$, and from the main reflector to the output constant-phase surface by the vector $\boldsymbol{M}$. The lengths of these vectors will be denoted as I, S, and M, respectively, and unit vectors along the rays will be written as $\hat{\boldsymbol{a}}_I$, $\hat{\boldsymbol{a}}_S$, and $\hat{\boldsymbol{a}}_M$, respectively. Let us suppose that the input constant-phase surface described by the vector $\boldsymbol{R}_I$ is parameterized by the variables u and v, and that the output surface described by the vector $\boldsymbol{R}_O$ is parameterized

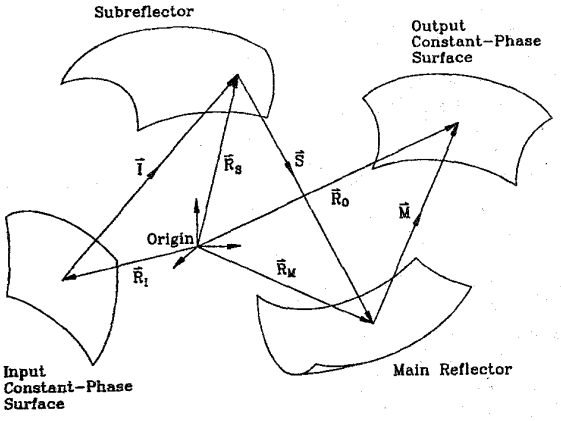

Fig. 2. Schematic diagram of a 3-D dual-shaped dual-reflector antenna system showing the surfaces involved in the derivation of the synthesis procedure.

by the variables μ and ν. It is assumed for simplicity that the (u, v) and (μ, ν) coordinates are each defined by orthogonal coordinate spaces.

We now apply Fermat's principle of stationary optical path length to the equation of total optical path length given by

$$I + S + M = L_T \tag{1}$$

where the constant L_T is the total optical path length. To apply the principle to the dual-reflector antenna system, we first hold a point on the main reflector fixed and take the partial derivatives of the equation of total optical path length with respect to the coordinates on the subreflector (actually, just two of the three coordinates, since only two are independent on the subreflector surface). Similarly, we hold a point on the subreflector fixed and take the partial derivatives with respect to two of the three main-reflector coordinates.

Applying Fermat's principle to the input coordinates and using the equation of total optical path length given in (1) yields

$$\frac{\partial}{\partial u}(I + S + M) = 0 \tag{2}$$

$$\frac{\partial}{\partial v}(I + S + M) = 0. \tag{3}$$

Here we assume that $\partial \boldsymbol{R}_M/\partial u = \partial \boldsymbol{R}_O/\partial u = 0$ and $\partial \boldsymbol{R}_M/\partial v = \partial \boldsymbol{R}_O/\partial v = 0$. In the derivation to follow we shall often make use of the following identity for an arbitrary vector $\boldsymbol{A}(u, v)$

$$\frac{\partial A}{\partial u} = \frac{\boldsymbol{A}}{A} \cdot \frac{\partial \boldsymbol{A}}{\partial u} \tag{4}$$

where $A = |\boldsymbol{A}|$. The result given in (4) may be obtained by differentiating $A = (\boldsymbol{A} \cdot \boldsymbol{A})^{1/2}$ with respect to u. A similar result holds for differentiation with respect to v. A study of Fig. 2 will show that $\boldsymbol{M}$ may be written as $\boldsymbol{M} = \boldsymbol{R}_O - \boldsymbol{R}_M$. Since $\partial \boldsymbol{R}_O/\partial u = \partial \boldsymbol{R}_M/\partial u = 0$, it follows that $\partial \boldsymbol{M}/\partial u = 0$. Using (4) with A = M then shows that $\partial M/\partial u = 0$. This

result is to be expected since we are holding the position on the main reflector fixed. For $\partial S/\partial u$, however, we find

$$\frac{\partial \boldsymbol{S}}{\partial u} = \frac{\boldsymbol{S}}{S} \cdot \frac{\partial \boldsymbol{S}}{\partial u} = \hat{\boldsymbol{a}}_{\boldsymbol{S}} \cdot \frac{\partial \boldsymbol{S}}{\partial u} = \hat{\boldsymbol{a}}_{\boldsymbol{S}} \cdot \frac{(\partial \boldsymbol{R}_{\boldsymbol{M}} - \boldsymbol{R}_{\boldsymbol{S}})}{\partial u} = -\hat{\boldsymbol{a}}_{\boldsymbol{S}} \cdot \frac{\partial \boldsymbol{R}_{\boldsymbol{S}}}{\partial u}. \tag{5}$$

The vector $\boldsymbol{R}_S$ may also be written as $\boldsymbol{R}_S = \boldsymbol{R}_I + \boldsymbol{I}$ so that

$$\frac{\partial \boldsymbol{S}}{\partial u} = -\hat{\boldsymbol{a}}_{\boldsymbol{S}} \cdot \left(\frac{\partial \boldsymbol{R}_{\boldsymbol{I}}}{\partial u} + \frac{\partial \boldsymbol{I}}{\partial u} \right). \tag{6}$$

If we let $\boldsymbol{I} = \hat{\boldsymbol{a}}_I \, \mathrm{I}$, we find

$$\frac{\partial \boldsymbol{I}}{\partial u} = \hat{\boldsymbol{a}}_{\boldsymbol{I}} \frac{\partial I}{\partial u} + I \frac{\partial \boldsymbol{a}_{\boldsymbol{I}}}{\partial u} \tag{7}$$

so that (5) may be written

$$\frac{\partial S}{\partial u} = -\hat{\boldsymbol{a}}_{\boldsymbol{S}} \cdot \frac{\partial \boldsymbol{R}_{\boldsymbol{I}}}{\partial u} - (\hat{\boldsymbol{a}}_{\boldsymbol{I}} \cdot \hat{\boldsymbol{a}}_{\boldsymbol{S}}) \frac{\partial I}{\partial u} - \left(\hat{\boldsymbol{a}}_{\boldsymbol{S}} \cdot \frac{\partial \boldsymbol{a}_{\boldsymbol{I}}}{\partial u} \right) I. \tag{8}$$

Equation (2) then becomes

$$\frac{\partial I}{\partial u} \neq -\hat{\boldsymbol{a}}_{\boldsymbol{S}} \cdot \frac{\partial \boldsymbol{R}_{\boldsymbol{I}}}{\partial u} - (\hat{\boldsymbol{a}}_{\boldsymbol{I}} \cdot \hat{\boldsymbol{a}}_{\boldsymbol{S}}) \frac{\partial I}{\partial u} - \left(\hat{\boldsymbol{a}}_{\boldsymbol{S}} \cdot \frac{\partial \boldsymbol{a}_{\boldsymbol{I}}}{\partial u} \right) I = 0. \tag{9}$$

Rearranging, we find

$$\frac{\partial I}{\partial u} = \frac{\hat{\boldsymbol{a}}_{\boldsymbol{S}} \cdot \left(\frac{\partial \boldsymbol{R}_I}{\partial u} + I \frac{\partial \hat{\boldsymbol{a}}_{\boldsymbol{I}}}{\partial u} \right)}{1 - \hat{\boldsymbol{a}}_{\boldsymbol{I}} \cdot \hat{\boldsymbol{a}}_{\boldsymbol{S}}}. \tag{10}$$

One may similarly show that

$$\frac{\partial I}{\partial v} = \frac{\hat{\boldsymbol{a}}_{\boldsymbol{S}} \cdot \left(\frac{\partial \boldsymbol{R}_I}{\partial v} + I \frac{\partial \hat{\boldsymbol{a}}_{\boldsymbol{I}}}{\partial v} \right)}{1 - \hat{\boldsymbol{a}}_{\boldsymbol{I}} \cdot \hat{\boldsymbol{a}}_{\boldsymbol{S}}}. \tag{11}$$

An analogous procedure applied to the output coordinates yields

$$\frac{\partial \boldsymbol{M}}{\partial \mu} = \frac{-\hat{\boldsymbol{a}}_{\boldsymbol{S}} \cdot \left(\frac{\partial \boldsymbol{R}_O}{\partial \mu} - M \frac{\partial \hat{\boldsymbol{a}}_{\boldsymbol{M}}}{\partial \mu} \right)}{1 - \hat{\boldsymbol{a}}_{\boldsymbol{S}} \cdot \hat{\boldsymbol{a}}_{\boldsymbol{M}}} \tag{12}$$

and

$$\frac{\partial M}{\partial \nu} = \frac{\hat{\boldsymbol{a}}_{\boldsymbol{S}} \cdot \left(\frac{\partial \boldsymbol{R}_O}{\partial \nu} - M \frac{\partial \hat{\boldsymbol{a}}_{\boldsymbol{I}}}{\partial \nu} \right)}{1 - \hat{\boldsymbol{a}}_{\boldsymbol{S}} \cdot \hat{\boldsymbol{a}}_{\boldsymbol{M}}}. \tag{13}$$

Note that at this point we have not yet defined the relationship between the (u, v) coordinates at the input and the (μ, ν) coordinates at the output. The transformations defined by $\mu = \mu(u, v)$ and $\nu = \nu(u, v)$ have generally been denoted in the literature as the "ray mapping." These functions may be determined as described in [6]. For our system we have obtained transformations such that $\mu = \mu(u)$ and $\nu = \nu(v)$.

Once the ray transformation has been determined, we begin the surface synthesis by specifying an initial point on each of the two reflectors. Since the transformation provides μ as a known function of u, the partial derivative $\partial \mathrm{M}/\partial \mu$ may be written as $\partial \mathrm{M}/\partial u$. We thus integrate both $\partial \mathrm{I}/\partial u$ and $\partial \mathrm{M}/\partial u$ along one of the constant v edges describing the input pupil. Given I and M along the initial edge, coordinates on each of the reflector edges may easily be determined. For example, the coordinates on the first reflector, or subreflector, are found from $\boldsymbol{R}_S = \boldsymbol{R}_I + \mathrm{I}\hat{\boldsymbol{a}}_I$. The points along these initial edges become the initial values for integration along the v-direction. Hence, across the interior of the input pupil, we integrate the partial differentials $\partial \mathrm{I}/\partial v$ and $\partial \mathrm{M}/\partial v$ (the latter obtained from $\partial \mathrm{M}/\partial \nu$ and the ray transformation $\nu = \nu(v)$).

IV. Synthesis Case Study

The synthesis method developed above will be illustrated by considering the transformation of the right-hand rotating $\mathrm{TE}_{15,2}$ mode in 50.8 mm (2 in) diameter waveguide at 110 GHz to the HE_{11} mode in 31.8 mm (1-1/4 in) diameter corrugated waveguide. At the system output, the beam is required to couple into an open-ended corrugated waveguide of 31.8 mm (1-1/4 in) diameter. The HE_{11} mode, which can be supported with low loss in this waveguide, is used to transport the microwave energy to the fusion experiment which may be several tens of meters from the gyrotron. The coupling efficiency is approximately maximized if the beam possesses the field structure of the TEM_{00}, or lowest-order Gaussian, free-space mode. The appropriate beam parameters for a given corrugated waveguide diameter have been considered in [7]. It was found that efficient coupling can be achieved if the 1/e-field radius is about 0.60 times the waveguide radius. In this case a 1/e-field diameter of 19.4 mm or about 7λ is easily large enough so that use of Gaussian beam expressions is justified. The Gaussian distribution required at the input to the corrugated waveguide was then traced back to a surface immediately following the main reflector to calculate the appropriate amplitude and phase of the GO rays used in the surface synthesis.

The overall conversion efficiency from the $\mathrm{TE}_{15,2}$ mode to the HE_{11} mode was somewhat enhanced by careful consideration of diffraction effects at the helically-cut waveguide which constituted the primary radiator in the reflector system. The GO-ray picture of the radiation of the $\mathrm{TE}_{15,2}$ mode from the waveguide was modified according to the results of a relatively simple diffraction analysis. A diffraction integral based on the vector Stratton–Chu formulation was used to predict the fields radiated from the helically-cut waveguide. A simple algebraic model, separable in two dimensions, was then fit to the calculated near-field patterns to more accurately account for the fields of the primary radiator.

The synthesized reflector shapes assuming the parameters specified above are shown in Figs. 3–5. A top view of the system, Fig. 3, illustrates the output beam focusing in the H-plane. Earlier versions of the Vlasov antenna had surface curvature in only two dimensions so that power shaping and focusing in the H-plane were not possible [5]. The profile of the main reflector is very nearly parabolic in the plane of the figure. This is rather obvious since the incident rays are approximately parallel and the output rays are focused to a single point. The side view shown in Fig. 4 illustrates the output beam focusing along the direction of polarization. From

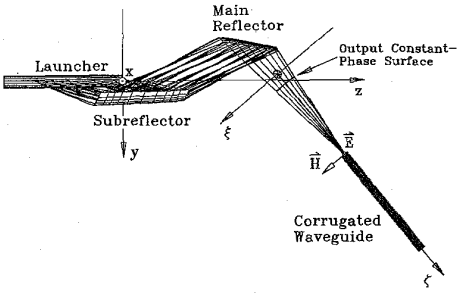

Fig. 3. Top view of the synthesized quasi-optical dual-shaped dual-reflector antenna system. The input waveguide has a 2 in (5.08 cm) diameter and 50 cm length, and all remaining elements of the system are drawn to scale.

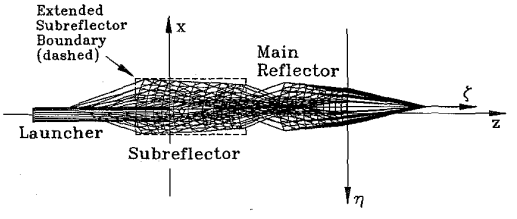

Fig. 4. Side view of the synthesized quasi-optical dual-shaped dual-reflector antenna system. Note that the projections of the boundaries of the reflectors onto the yz-plane (the plane parallel to the page) are not perfectly rectangular.

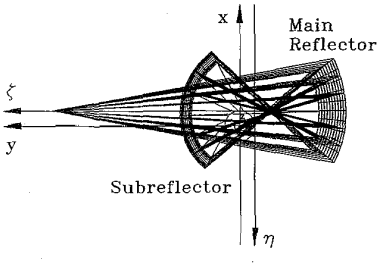

Fig. 5. End view of the synthesized quasi-optical dual-shaped dual-reflector antenna system.

this figure we also see that the projections of the reflectors onto the xz-plane are almost rectangular which follows from the shapes of the input and output pupils. The sizes of the sub- and main reflectors may also be considered from this perspective. The subreflector is roughly 40 cm by 20 cm, or 147λ by 73λ. The main reflector is roughly 26 cm by 18 cm, or 95λ by 66λ. The large reflector dimensions relative to λ and the slowly varying reflector curvatures are positive justification for using GO surface-shaping techniques. The end view of the system given in Fig. 5 also shows the output beam focusing along the direction of polarization.

V. Experimental Results

The complete reflector system was first investigated at low power (a few mW) to allow for safe and accurate near-field radiation pattern measurement. The source of right-hand rotating $TE_{15,2}$ mode was a low-power mode transducer designed by Moeller at General Atomics [8]. Open-end waveguide radiation pattern measurements indicate that the output mode

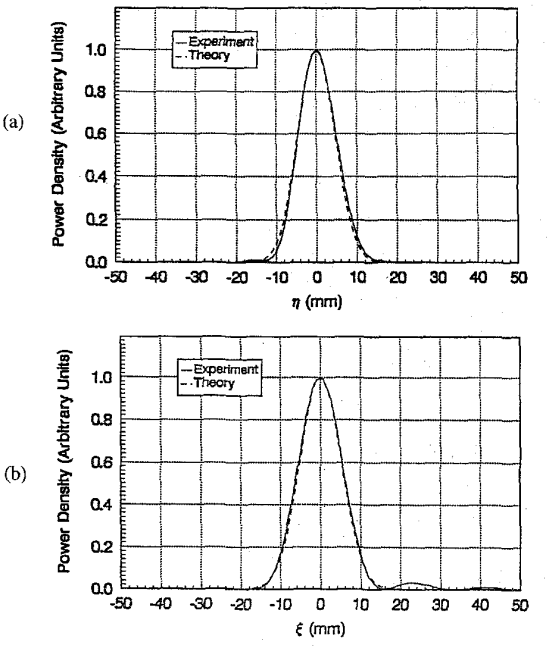

Fig. 6. Gaussian distributions fit to the measured E- and H-plane field patterns at the beam waist (ζ - ζ_o = 0). (a) E-plane fit. (b) H-plane fit. Note that the right-side lobe appearing in the measured field pattern may be due to the presence of spurious modes (probably $TE_{16,2}$) in the field radiated by the launcher.

purity of this transducer is about 99% with approximately 0.5% impurity in the left-hand rotating $TE_{15,2}$ mode and 0.5% in other modes.

The radiation pattern following the main reflector was measured both before and after coupling into a length of corrugated waveguide. The measurements were made with an open-ended F-band waveguide used as the receiving element in a heterodyne detection system. A comparison of an exact Gaussian power distribution and the measured power densities at the beam waist are shown in Fig. 6. The side lobe observed in the H-plane may be due to the presence of a spurious mode coming from the mode transducer or generated at the junctions of the highly-overmoded waveguide components (recall that over 800 modes can propagate in the 50.8 mm diameter waveguide at 110 GHz). Analogous observations have been made by others working on similar devices [3]. The measured cross-polarization at the beam waist was less than -25 dB. The theoretical and measured 1/e-field radii and on-axis power density are plotted as a function of the length along the axis of the output beam in Figs. 7 and 8. The results indicate that a substantially pure output Gaussian beam has been achieved.

The beam was then coupled into the open end of a section of 1-1/4 in (3.18 cm) diameter corrugated waveguide. The radiation pattern taken at a distance of 1 m from the open end of the waveguide is shown in Fig. 9. Note that over 99% of the power in the HE_{11} mode is contained in the radiation pattern above the level of -20 dB. The measured cross polarization is also quite low, in substantial agreement with the theoretical prediction that cross-polarization vanishes in the plane of the measurement.

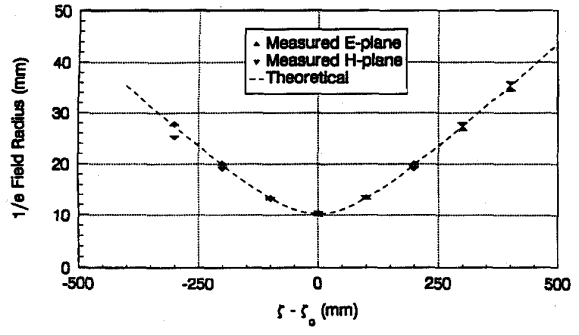

Fig. 7. Measured and theoretical E- and H-plane 1/e-field radii. The theoretical curve assumes a Gaussian power distribution.

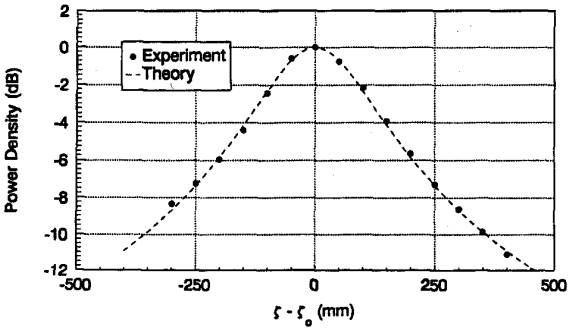

Fig. 8. Measured and theoretical power densities along the axis of the output beam. The theoretical curve assumes a Gaussian power distribution.

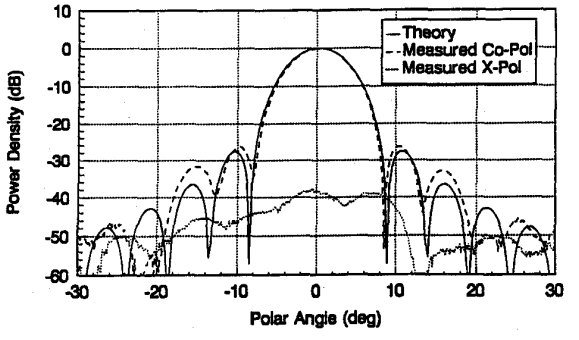

Fig. 9. Theoretical copolarization and measured co- and cross-polarizations of the far-field radiation patterns following the open-ended corrugated waveguide. The theory assumes a pure HE_{11} mode.

The system of reflectors and input and output waveguides have been mounted and aligned as a single unit. High-power testing at about 300 to 350 kW using a TE $_{15,2}$ mode gyrotron manufactured by Varian Associates of Palo Alto, California was performed at General Atomics in San Diego, California. The mode purity of the gyrotron was measured using a phase-velocity coupler which is similar to the slotted waveguide described as an element in the system appearing in [9]. The average value of coupling from the $TE_{15,2}$ mode to the corrugated waveguide was determined to be over 94% with about 4% standard deviation in the measured results. This value should be compared to coupling efficiencies of about 80% reported in [1] for the original class of reflector system upon which our fully 3-D (doubly-curved reflectors) system is based. A somewhat improved two-dimensional version (singly-curved reflectors) of the original device reportedly generated an output beam in which about 93% of the power was contained in the main lobe of the radiation pattern [10]. No value was reported for coupling of this main lobe to either a Gaussian beam or the HE_{11} mode.

VI. Conclusion

We have described a dual-shaped dual-reflector synthesis procedure which is a recasting of a well-established technique used for the design of reflector antennas with applications in satellite communications, radio astronomy, etc. The primary radiator considered cannot conveniently be described as a point source, nor was the input pupil circular in shape. In addition, a focused output beam was required so that the field could be coupled into an open-ended waveguide.

The synthesis technique was applied to the design of a dual-shaped dual-reflector antenna system for the transformation of the right-hand rotating $TE_{15,2}$ mode in 50.8 mm (2 in) diameter waveguide at 110 GHz into the HE_{11} mode in 31.8 mm (1-1/4 in) diameter corrugated waveguide. A set of reflectors was fabricated and tested using a low-power mode transducer. The measured results showed excellent agreement with theory verifying the surface shaping technique which we have presented.

Acknowledgment

The authors gratefully acknowledge the use of the low-power mode transducer designed by C. Moeller at General Atomics.

References

[1] S. N. Vlasov, L. I. Zagryadskaya, and M. I. Petelin, "Transformation of a whispering gallery mode, propagating in a circular waveguide, into a beam of waves," *Radio Eng. Electron. Phys.*, vol. 21, no. 10, pp. 14–17, 1975.

[2] O. Wada, M. Hashimoto, and M. Nakajima, "Calculation of radiation from a quasi-optical reflector antenna for whispering gallery mode," *Int. J. Electron.*, vol. 65, no. 3, pp. 725–732, 1988.

[3] M. Blank, J. A. Casey, K. E. Kreischer, R. J. Temkin, and T. Price, "Experimental study of a high efficiency quasi-optical antenna for whispering gallery mode gyrotrons," *Int. J. Electronics*, vol. 72, no. 5, 1992.

[4] V. Galindo-Israel, R. Mittra, and A. G. Cha, "Aperture amplitude and phase control of offset dual reflectors," *IEEE Trans. Antennas Propagat.*, vol. AP-27, no. 2, pp. 154–164, Mar. 1979.

[5] J. A. Lorbeck and R. J. Vernon, "Singly curved dual-reflector synthesis technique applied to a quasi-optical antenna for a gyrotron with a whispering-gallery mode output," *IEEE Trans. Antennas Propagat.*, vol. 39, no. 12, pp. 1733–1741, Dec. 1991.

[6] P. S. Kildal, "Laws of geometrical optics mapping in multi-reflector antennas with application to elliptical apertures," *IEE Proc.*, vol. 136, pt. H, no. 6, pp. 445–451, Dec. 1989.

[7] L. Rebuffi and J. P. Crenn, "Radiation patterns of the HE_{11} mode and Gaussian approximations," *Int. J. Infrared Millimeter Waves*, vol. 10, no. 3, pp. 291–311, Mar. 1989.

[8] C. P. Moeller, "A coupled cavity whispering-gallery mode transducer," in *Conf. Dig. 17th Int. Conf. Infrared Millimeter Waves*, pp. 42–43, Pasadena, CA, 1992.

[9] C. P. Moeller and J. L. Doane, "Coaxial converter for transforming a whispering gallery mode to the HE_{11} mode," in *Conf. Dig. 15th Int. Conf. Infrared Millimeter Waves,* pp. 213–215, Orlando, FL, 1990.

[10] M. Iima *et al.*, "Measurement of radiation field from an improved efficiency quasi-optical converter for whispering-gallery mode," in *Conf. Dig. 14th Int. Conf. Infrared Millimeter Waves,* pp. 405–406, Wurtzburg, Germany, 1989.

Jeffrey A. Lorbeck (S'89–M'93) was born in Milwaukee, WI, on December 30, 1963. He received the B.S., M.S., and Ph.D. degrees in electrical engineering from the University of Wisconsin, Madison, in 1987, 1988, and 1992, respectively.

He is currently working at QUALCOMM, Inc.

Dr. Lorbeck received the Magnetic Fusion Energy Technology Fellowship from the U.S. Department of Energy by Oak Ridge Associated Universities.

Ronald J. Vernon (S'64–M'65) was born in Chicago, IL, on June 3, 1936. He received the B.S., M.S., and Ph.D. degrees in electrical engineering from Northwestern University, Evanston, IL, in 1959, 1961, and 1965, respectively.

He worked under a cooperative student program in the Remote Control Engineering Division of Argonne National Laboratory from 1955 to 1958. Since 1965, he has been on the faculty of the University of Wisconsin, Madison, where he is currently a Professor of Electrical and Computer Engineering and directs a graduate research program in the area of microwaves and electromagnetic wave propagation. From 1976–1977 he took a leave of absence to work at Lawrence Livermore National Laboratory. His current research interests are in the development of transmission and mode conversion systems and beam-shaping reflector antennas for high-power microwave tubes such as gyrotrons.

Dr. Vernon is a member of Sigma Xi, Tau Beta Pi, Eta Kappa Nu, and Pi Mu Epsilon.